1-1-2008

Femtosecond laser photo-response of Ge23Sb7S70 films

Troy Anderson
University of Central Florida

Laeticia Petit

Nathan Calie

Jiyeon Choi
University of Central Florida

Juejun Hu

See next page for additional authors

Femtosecond laser photo-response of $Ge_{23}Sb_7S_{70}$ films

Troy Anderson[1*], Laeticia Petit[2], Nathan Carlie[2], Jiyeon Choi[1], Juejun Hu[3], Anu Agarwal[3], Lionel Kimerling[3], Kathleen Richardson[2], Martin Richardson[1]

[1]*College of Optics/CREOL, University of Central Florida, 4000 Central Florida Blvd., Orlando, FL 32816, USA*
[2]*Advanced Materials Research Laboratory, Clemson University, 91 Technology Dr., Anderson, SC 29625, USA*
[3]*Microphotonics Center, MIT, Cambridge, MA 02139, USA*
[*]*Corresponding Author: troy@creol.ucf.edu*

Abstract: Ternary chalcogenide glass films from identical parent bulk glasses were prepared by thermal evaporation (TE) and pulsed laser deposition (PLD) and subjected to 810-nm femtosecond laser exposure at both kHz and MHz repetition rates. The exposure-induced modification on the glass film's surface profile, refractive index, and structural properties were shown to be a function of laser irradiance, the number of laser pulses per focal spot, and repetition rate. Film response was shown to be related to deposition technique-related density and the number of glass bonds within the irradiated focal volume. The induced changes resulted from a reduction in glass network connectivity among $GeS_{4/2}$, GeS_4, S-S and S_3Ge-S-GeS_3 units.

OCIS codes: (140.3390) Laser materials processing; (320.2250) Femtosecond phenomena; (300.6450) Spectroscopy, Raman; (160.4760) Optical properties; (240.0310) Thin films.

References and links

1. K. M. Davis, K. Miura, N. Sugimoto, and K. Hirao, "Writing waveguides in glass with a femtosecond laser," Opt. Lett. **21**, 1729-1731 (1996).
2. S. Nolte, M. Will, J. Burghoff, and A. Tünnermann, "Femtosecond waveguide writing: a new avenue to three-dimensional integrated optics," Appl. Phys. A **77**, 109-111 (2003).
3. C. B. Schaffer, A. Brodeur, J. F. Garcia, and E. Mazur, "Micromachining bulk glass by use of femtosecond laser pulses with nanojoule energy," Opt. Lett. **26**, 93-95 (2001).
4. O. M. Efimov, L. B. Glebov, K. A. Richardson, E. V. Stryland, T. Cardinal, S. H. Park, M. Couzi, and J. L. Brunéel, "Waveguide writing in chalcogenide glasses by a train of femtosecond laser pulses," Opt. Mat. **17**, 379-386 (2001).
5. A. Zoubir, M. Richardson, C. Rivero, A. Schulte, C. Lopez, K. Richardson, N. Hô, and R. Vallée, "Direct femtosecond laser writing of waveguides in As2S3 thin films," Opt. Lett. **29**, 748-750 (2004).
6. A. Schulte, C. Rivero, K. Richardson, K. Turcotte, V. Hamel, A. Villeneuve, T. Galstian, and R. Vallee, "Bulk-film structural differences of chalcogenide glasses probed in situ by near-infrared waveguide Raman spectroscopy," Opt. Commun. **198**, 125-128 (2001).
7. J. W. Chan, T. Huser, S. Risbud, J. S. Hayden, and D. M. Krol, "Waveguide fabrication in phosphate glasses using femtosecond laser pulses," Appl. Phys. Lett. **82**, 2371-2373 (2003).
8. T. Cardinal, K. A. Richardson, H. Shim, A. Schulte, R. Beatty, K. L. Foulgoc, C. Meneghini, J. F. Viens, and A. Villeneuve, "Non-linear optical properties of chalcogenide glasses in the system As-S-Se," J. Non-Cryst. Solids **256-257**, 353-360 (1999).
9. J. M. Laniel, J. Ménard, K. Turcotte, A. Villeneuve, R. Vallée, C. Lopez, and K. Richardson, "Refractive index measurements of planar chalcogenide thin film," J. Non-Cryst. Solids **328**, 183-191 (2003).
10. W. Li, S. Seal, C. Rivero, C. Lopez, K. Richardson, A. Pope, A. Schulte, S. Myneni, H. Jain, K. Antoine, and A. C. Miller, "Role of S/Se ratio in chemical bonding of As-S-Se glasses investigated by Raman, x-ray photoelectron, and extended x-ray absorption fine structure spectroscopies," J. Appl. Phys. **98**, 053503 (2005).
11. A. B. Seddon, "Chalcogenide glasses: a review of their preparation, properties, and applications," J. Non-Cryst. Solids 184, **44** (1995).
12. A. Zoubir, L. Shah, K. Richardson, and M. Richardson, "Practical uses of femtosecond laser micro-materials processing," Appl. Phys. A **77**, 311-315 (2003).

#100939 - $15.00 USD Received 8 Sep 2008; revised 3 Nov 2008; accepted 7 Nov 2008; published 21 Nov 2008

13. N. J. Baker, H. W. Lee, I. C. Littler, C. M. de Sterke, B. J. Eggleton, D. Y. Choi, S. Madden, and B. Luther-Davies, "Sampled Bragg gratings in chalcogenide (As2S3) rib-waveguides," Opt. Express **14**, 9451-9459 (2006).
14. E. Verpoorte and N. D. Rooij, "Microfluidics meets MEMS," Proc. IEEE **91**, 930-953 (2003).
15. P. Friis, K. Hoppe, O. Leistiko, K. B. Mogensen, J. Hübner, and J. P. Kutter, "Monolithic integration of microfluidic channels and optical waveguides in silica on silicon," Appl. Opt. **40**, 6246-6251 (2001).
16. N. Petersen, K. Mogensen, and J. P. Kutter, "Performance of an in-plane detection cell with integrated waveguides for UV/VIS absorbance measurements on microfluidic separation devices," Electrophoresis **23**, 3528-3536 (2002).
17. Z. Sun, J. Zhou, and R. Ahuja, "Structure of phase change materials for Data Storage," Phys. Rev. Lett. **96**, 055507 (2006).
18. L. Zan, L. Huang, and C. Zhang, "New chalcogenide glasses from the Sb_{2}S_{3}-MXn system," J. Non-Cryst. Solids **184**, 1-4 (1995).
19. E. N. Kotlokov and G. V. Tereshchenko, "The use of chalcogenide compounds for fabricating antireflection coatings in the mid-IR region," J. Opt. Technol. **64**, 264-268. (1997).
20. D. A. C. Compton, S. L. Hill, N. A. Wright, M. A. Druy, J. Piche, W. A. Stevenson, and D. W. Vidrine, "In Situ FT-IR Analysis of a Composite Curing Reaction using a Mid-Infrared Transmitting Optical Fiber," Appl. Spectrosc. **42**, 972-979 (1998).
21. J. S. Sanghera, F. H. Kung, P. C. Pureza, V. Q. Nguyen, R. E. Miklos, and I. D. Aggarwal, "Infrared Evanescent-Absorption Spectroscopy with Chalcogenide Glass-Fibers," Appl. Opt. **33**, 6315-6322 (1994).
22. P. Lucas, M. A. Solis, D. Le Coq, C. Juncker, M. R. Riley, J. Collier, D. E. Boesewetter, C. Boussard-Plédel, and B. Bureau, "Infrared biosensors using hydrophobic chalcogenide fibers sensitized with live cells," Sensor Actuator B **119**, 355-362 (2006).
23. J. Hu, V. Tarasov, A. Agarwal, L. Kimerling, N. Carlie, L. Petit, and K. Richardson, "Fabrication and Testing of Planar Chalcogenide Waveguide Intregrated Microfluidic Sensor," Opt. Express **15**, 2307 (2007).
24. J. F. Viens, C. Meneghini, A. Villeneuve, T. V. Galstian, E. J. Knystautas, M. A. Duguay, K. A. Richardson, and T. Cardinal, "Fabrication and characterization of integrated optical waveguidesin sulfide chalcogenide glasses," J. Lightwave Technol. **17**, 1184-1191 (1999).
25. Y. Ruan, W. Li, R. Jarvis, N. Madsen, A. Rode, and B. Luther-Davies, "Fabrication and characterization of low loss rib chalcogenide waveguides made by dry etching," Opt. Express **12**, 5140-5145 (2004).
26. J. Hu, V. Tarasov, N. Carlie, N. Feng, L. Petit, A. Agarwal, K. Richardson, and L. Kimerling, "Si-CMOS-compatible lift-off fabrication of low-loss planar chalcogenide waveguides," Opt. Express **15**, 11798 (2007).
27. L. Petit, N. Carlie, T. Anderson, M. Couzi, J. Choi, M. Richardson, and K. C. Richardson, "Effect of IR femtosecond laser irradiation on the structure of new sulfo-selenide glasses," Opt. Mater. **29**, 1075-1083 (2007).
28. B. Luther-Davies, V. Z. Kolev, M. J. Lederer, N. R. Madsen, A. V. Rode, J. Giesekus, K. M. Du, and M. Duering, "Table-top 50W laser system for ultra-fast ablation," Appl. Phys. A **79**, 1051-1055 (2004).
29. R. Swanepoel, "Determination of the thickness and optical constants of amorphous silicon," J. Phys. E **16**, 1214-1222 (1983).
30. B. Frumarova, P. Nemec, M. Frumar, J. Oswald, and M. Vlcek, "Synthesis and optical properties of the Ge-Sb-S:PrCl_{3} glass system," J. Non-Cryst. Solids **256-257**, 266-270 (1999).
31. Q. Mei, J. Saienga, J. Schrooten, B. Meyer, and S. W. Martin, "Preparation and characterization of glasses in the Ag_{2}S+B_{2}S_{3}+GeS_{2} system," J. Non-Cryst. Solids **324**, 264-276 (2003).
32. C. Julien, S. Barnier, M. Massot, N. Chbani, X. Cai, A. M. Loireau-Lozac'h, and M. Guittard, "Raman and infrared spectroscopic studies of Ge---Ga---Ag sulphide glasses," Mater. Sci. Eng. B **22**, 191-200 (1994).
33. T. Wagner, "Pulsed laser deposition of Ge_{2}Sb_{2}Te_{5} plume particle analysis and properties of prepared thin films," in *International Symposium on Non-Oxide Glasses*, 2008), IC13.
34. M. Born and E. Wolf, *Principles of Optics*, Seventh (Expanded) ed. (Cambridge University Press, Cambridge, UK, 1999).
35. C. Z. Tan and J. Arndt, "The mean polarizability and density of glasses," Physica B **229**, 217-224 (1997).
36. S. H. Messaddeq, M. S. Li, D. Lezal, S. J. L. Ribeiro, and Y. Massaddeq, "Above bandgap induced photoexpansion and photobleaching in Ga-Ge-S based glasses," J. Non-Cryst. Solids **284**, 282-287 (2001).
37. J. Tasseva, K. Petkov, D. Kozhuharova, and T. Iliev, "Light-induced changes in the physico-chemical and optical properties of thin Ge-S-Se-As films," J. Optoelectron. Adv. M. **7**, 1287-1292 (2005).
38. V. Lyubin, M. Klebanov, I. Bar, S. Rosenwaks, V. Volterra, L. Boehm, and Z. Vagish, "Laser-induced phenomena in chalcogenide glassy films," Appl. Surf. Sci. **106**, 502-506 (1996).
39. K. Tanaka, "Spectral dependence of photoexpansion in As_{2}S_{3} glass," Philos. Mag. Lett. **79**, 25-30 (1999).
40. K. Tanaka and H. Hisakuni, "Photoinduced phenomena in As2S3 glass under sub-bandgap excitation," J. Non-Cryst. Solids **198-200**, 714-718 (1996).
41. S. R. Elliott, "A unified model for reversible photostructural effects in chalcogenide glasses," J. Non-Cryst. Solids **81**, 71-98 (1986).
42. P. Loeffler, T. Schwarz, H. Sautter, and D. Lezal, "Structural changes of GeGaS bulk glasses induced by UV exposure," J. Non-Cryst. Solids **232-234**, 526-531 (1998).

#100939 - $15.00 USD Received 8 Sep 2008; revised 3 Nov 2008; accepted 7 Nov 2008; published 21 Nov 2008

43. S. H. Messaddeq, V. R. Mastelaro, M. S. Li, M. Tabackniks, D. Lezal, A. Ramos, and Y. Messaddeq, "The infludence of oxygen in the photoexpansion of GaGeS glasses," Appl. Surf. Sci. **205**, 143-150 (2003).

1. Introduction

Femtosecond direct-writing using laser pulses with both kHz and MHz repetition rate pulses is well established as a method of fabricating photonic structures in amorphous materials such as silica, phosphate, and chalcogenide glasses [1-7]. While much research has been done to understand and control the induced material modifications in these glasses, it is still difficult to predict *a priori* the response of an unstudied material to IR femtosecond irradiation. Therefore, the response of a new material of interest to IR femtosecond irradiation should be thoroughly characterized before optimized structures can be fabricated.

Chalcogenide glasses (ChGs) have attracted the attention of many investigators due to their chemical and structural flexibility, good IR transparency, high optical nonlinearity, and high photosensitivity [8]. In comparison with oxide glasses and single crystals, ChGs have an advantage in that they exhibit wide refractive index variation with chemical composition and can readily be compositionally tailored to optimize other physical and optical properties [9-11]. For these reasons, ChGs, primarily As_2S_3, have been used in applications such as gratings [12-14], optical storage [15], as holographic recording media [16], optical amplifiers and lasers [17], and antireflection coatings [18, 19]. Additionally, their wide transparency window stretching from the visible to the far-infrared makes chalcogenide glasses ideal candidates for integrated optical circuits including optical waveguides, and can be considered for *lab-on-a-chip* applications for chemical and biological sensing where their transparency in the mid- and far-infrared fingerprint regions of many chemicals and biological toxins make them attractive [20-23]. Compared to their fiber-form counterparts, planar ChG-based structures are more versatile and amenable to large-scale integration with other on-chip photonic and electronic devices, enabling a full spectrum of optical function (splitters, routers, switches, lenses and filters) as well as signal read-out and processing functions.

Germanium-based chalcogenide waveguides containing heavy metal species have been fabricated in several glass compositions using techniques including wet etching [24], plasma etching [23, 25], and lift-off [26]. Recently, we have shown the successful fabrication of chalcogenide waveguides in these films with a minimum loss of 2.3 dB/cm in the film using SF_6 plasma etching, which is intended to be used as an evanescent sensor integrated with microfluidic channels for analyte transport [23]. Additionally, we have previously shown that bulk $Ge_{23}Sb_7S_{70}$ glass is photo-sensitive to IR femtosecond laser exposure and exhibits a dose-dependant surface photo-expansion up to (350±5) nm when exposed to IR femtosecond laser pulses at a repetition rate of 35.8 MHz [27].

In this paper, the photo-induced modification of the refractive index (Δn), surface profile modification (as characterized by laser-induced photo-expansion, ΔT), and structural (bonding) changes in glassy of $Ge_{23}Sb_7S_{70}$ thin films exposed to 810 nm femtosecond laser pulses has been investigated as a function of exposure conditions (number of pulses per focal spot and laser irradiance). Two irradiation regimes have been examined to elucidate the influence of incubation effects on material photo-response: 80MHz repetition rate pulses with nanojoule energies and a 1kHz repetition rate pulses with microjoule energies. In each regime, the induced photo-expansion (ΔT) and refractive index change (Δn) has been measured. Micro-Raman spectroscopy has been used to define the mechanism of the film's structural modifications as a result of laser irradiation. Understanding the relationship between the optical properties and the physical modifications of the ChG film following laser exposure is a prerequisite for the development of new ChGs with optimized compositions suitable for successful use in the development of photonic devices using femtosecond direct laser writing.

#100939 - $15.00 USD Received 8 Sep 2008; revised 3 Nov 2008; accepted 7 Nov 2008; published 21 Nov 2008

2. Experimental setup

2.1 Film deposition

Chalcogenide glass thin films from parent bulk glasses of composition $Ge_{23}Sb_7S_{70}$ were deposited using thermal evaporation (TE) and pulsed laser deposition (PLD) techniques. The deposition of the investigated films was carried out using the same parent glass as targets: for TE film deposition, bulk glass was ground into glass powder whereas polished bulk glass targets at least 2 cm in diameter and 3 mm in thickness were used for PLD film deposition. The bulk glasses used as targets for the film deposition were prepared in separate batches of 6 g for TE and 50 g for PLD, using identical melting conditions. Although the melt volumes varied, yielding slightly different thermal histories, the resulting bulk glass physical properties were identical. Bulk glasses were prepared from high purity elements (Ge: Aldrich 99.999%, Sb: Alpha 99.9% and S: Cerac 99.999%). The starting materials were weighed and batched into quartz ampoules inside a nitrogen-purged glove box. Prior to sealing and melting, the quartz ampoules and batch raw materials were pre-heated at 100°C for 4 hours to remove surface moisture. The ampoules were then sealed under vacuum with a gas-oxygen torch and heated to 975°C for 15 to 24 hours, depending on the weight of the batch to melt. A rocking furnace was used to rock each ampoule while melting to increase the homogeneity of the melt. Once homogenized, the ampoules were air-quenched to room temperature. To avoid fracture of the tube and glass ingot, the ampoules were subsequently returned to the furnace for annealing for 15 hours at 40°C below the glass transition temperature, T_g.

2.1.1 Thermal Evaporation technique for deposition of the TE film

Thermal evaporation of the ChG glass films was performed at a base pressure of $< 10^{-6}$ Torr using a Tantalum baffled source, and the deposition rate was stabilized at approximately 2 nm/s. A thermostat stage was employed to maintain the substrate temperature at 25 °C throughout the deposition process.

2.1.2 Pulsed Laser Deposition technique for deposition of the PLD film

Pulsed laser deposition was performed using a mode-locked Nd:YVO_4 laser operating at third harmonic (355 nm) and delivering ~5 W to the polished glass target surface [28]. The laser repetition rate was 28 MHz, the pulse duration 12 ps, the focal spot size ~ 15 μm, and the maximum incident intensity was $\sim 10^{10}$ W/cm^2 with a fluence of 0.1 J/cm^2. The laser beam was scanned across the 2 cm diameter ChG target using x-y scanning mirrors in a constant velocity 2 m/s spiral over an area of approx. 2.5 cm^2 to prevent drilling craters into the target surface. The substrate was located ~160 mm from the target and rotated to provide a more homogeneous film thickness over the substrate area. The base pressure in the deposition chamber was 5.0×10^{-7} Torr.

The TE and PLD films were deposited onto glass microscope slide substrates and had thicknesses of (1.4±0.1) μm and (1.0±0.1) μm, respectively, measured using a scanning electron microscope (SEM) and confirmed with Zygo 3D Optical Profiler. The films did not display any evidence of crystallization or phase separation. The films did not undergo an immediate post-deposition annealing, but all exposure studies were carried out months after film deposition where extensive film relaxation was confirmed to have occurred.

2.2 Femtosecond laser sources

Two 810 nm femtosecond lasers with 80 MHz (KMLabs, Inc) and 1 kHz (Spitfire, Spectra Physics) repetition rates were used as irradiation sources to study incubation effects associated with femtosecond processing in the glass films. The laser pulse energies used in this experiment were on the order of nanojoules for the MHz laser and microjoules for the kHz laser. The MHz oscillator also served as the seed laser for the amplified system. These lasers produced 120 femtosecond pulses with a ~13 nm spectral bandwidth and 5% pulse-to-pulse

#100939 - $15.00 USD Received 8 Sep 2008; revised 3 Nov 2008; accepted 7 Nov 2008; published 21 Nov 2008

stability. A 0.25NA microscope objective was used to focus the laser light onto the samples, which were mounted on a computer-controlled 3D translation stage (VP-25XA, Newport). Spots or squares of irradiated regions were generated in the film surface depending on the post-exposure analysis to be performed.

2.3 Ablation threshold

The first metric used to compare the photo-response of the two films was the determination of the ablation threshold of each film. Previous work by our group has used this metric to directly compare the response of bulk and films of ChG and other glass materials to assess photo-induced material response (induced expansion, contraction or ablation) [27]. This threshold was determined in ChG films in this study by fabricating a spatial two dimensional map on the film surface consisting of a series of photo-written lines with a large number of pulses per focal spot (198 and $4 \cdot 10^6$ for the kHz and MHz repetition rates, respectively) and increasing laser irradiance. The ablation threshold determined from the resulting exposure map is defined as the onset of the exposure region where the laser irradiance was sufficient to result in ablation of film material. This response was accompanied by the formation of a trench that could be observed by measuring the surface profile of the films after irradiation using a Zygo NewView 6300 3D Optical Profilometer. The corresponding number of pulses per focal spot for each repetition rate associated with this transition region (threshold) for kHz and MHz exposure conditions varies for all materials, and in this study the threshold, were defined as the upper bound of exposure conditions for each material to assess resulting photo-expansion and refractive index change.

2.4 Photo-expansion (ΔT)

Two series of lines with varying laser exposure conditions were fabricated on each type of film using both kHz and MHz repetition rate pulses to analyze the effect of exposure parameters on the film's post-exposure surface morphology. In the first series, the number of pulses per focal spot was held constant and the laser irradiance was varied, while in the second, the laser irradiance was fixed and the number of pulses per focal spot was varied. The resulting post-exposure film surface profiles were measured obtained using both a Zygo 3D Optical Profiler and a μTA-2990 from TA Instruments used as an AFM. Surface images were digitally leveled and the heights of 3 points on each irradiated line were averaged to calculate a measurement of the photo-expansion. The measurements using the two instruments were found to be in agreement within the accuracy of the measurements, ±0.7 nm.

2.5 Refractive index modification (Δn)

The photo-induced refractive index modification of the glass films has been measured by analyzing i) the pre- and post-exposure transmission spectra using a spectrophotometer and assessing the resulting spectra using the method published by Swanepoel [29] and by ii) quantifying the optical path changes using a Zygo NewView 6300 3D Optical Profilometer and calculating the induced phase shift in the exposed region [5].

Transmission spectrophotometry was used to determine the refractive index of an irradiated region of material as a function of wavelength in the transparent spectral region of the glass. A 1.2 mm x 1.2 mm irradiated square region consisting of parallel lines separated by 2 μm was fabricated so that the entire area probed by the spectrometer was exposed. A Cary 500 spectrophotometer from Varian was then used to measure the transmission spectrum in the range 800 to 1500nm of the square region before and following laser irradiation. It is well known that transmission spectra of a thin film contains a periodic variation of the transmission as a function of wavelength due to interference caused by reflections at the two surfaces of the film. Both the film thickness and the refractive index of the film influence the interference pattern and can be calculated using an analysis of the film transmission as a function of

#100939 - $15.00 USD Received 8 Sep 2008; revised 3 Nov 2008; accepted 7 Nov 2008; published 21 Nov 2008

wavelength described by Swanepoel [29]. The accuracy of the refractive index and thickness measurement were estimated to be ±0.02 and ±5 nm, respectively.

The second technique involved use of white light interferometry with a Zygo 3D Optical Profiler to measure the exposure-induced refractive index changes for of series of lines prepared using the method described in Section 2.4. In contrast to the previous technique, white light interferometry possesses adequate spatial resolution to measure the refractive index variation of single irradiated lines at the expense of the spectral wavelength resolution. The white light source used for this experiment had a bandwidth 100 nm centered at 550 nm. An interference pattern is created by combining light reflected from the film/substrate interface with a reference beam to produce a series of Fizeau fringes. Any change of the optical path is manifested as a phase shift in the interference pattern. This phase shift can be related to the refractive index by

$$\frac{\Delta\varphi}{2\pi} = \frac{2\cdot\left(n_{irr}d_{irr} - n_0 d_0\right)}{\bar{\lambda}} \tag{1}$$

where $\Delta\varphi$ is the induced phase shift, $\bar{\lambda}$ is the average wavelength of the white light source (estimated at 550nm), n is the refractive index, and d is the film thickness. The refractive index, n_0, and thickness, d_0 of the unirradiated film were obtained using the Swanepoel technique. The thickness, d_{irr}, of the irradiated film was calculated by adding the exposure-induced expansion measured with the Zygo 3D Optical Profilometer (photo-expansion) and the TA Instruments model 2990 micro-thermal analyzer (μTA) used an AFM, to the thickness of the unirradiated film. The accuracy of the measurement was limited by the accuracy of unirradiated film index as determined using the Swanepoel method, estimated to be ± 0.02.

2.6 Structural characterization

The Raman spectra of pre- and post-exposed films were recorded using a Kaiser Hololab 5000R Raman spectrometer. This system has a typical resolution of 2-3 cm^{-1} at room temperature and uses a backscattering geometry. The system consists of a holographic notch filter for Rayleigh rejection, a microscope equipped with 10x, 50x and 100x objectives and a CCD detector. A 785 nm NIR semiconductor diode laser was used for excitation. This wavelength was chosen specifically for this study to reduce absorption and photo-structural changes during the measurement.

3. Results and discussion

Before discussing the variation of the Raman spectra of the films as a function of laser irradiation, a brief description of the as-deposited film structural characteristics is presented. The Raman spectra of these unirradiated TE and PLD films are shown in Fig. 1. These spectra have been deconvolved into the Raman bands of the constituent vibrational modes of the molecules in the glass matrix using the same method used previously for the Raman spectra of bulk glasses in the Ge-Sb-S-Se family [27]. The Raman spectrum of the non-irradiated films consists of a broad band from 275-450cm^{-1} and two low-amplitude bands in the 200-250 and 450-550 cm^{-1} range. The main band is formed by the overlapping of the Raman bands of Sb_2S_3, GeS_2 and S_n structural units. The shoulder at around 302 cm^{-1} has been assigned to the E modes of SbS_3 pyramids [30]. In accordance with Mei *et al*, the bands at 330 and 402 cm^{-1} have been assigned to the A_1 and T_2 modes of corner sharing $GeS_{4/2}$ groups [31]. The bands at 340, 375 and 427 cm^{-1} have been attributed, respectively to the A_1 mode of the GeS_4 molecular units [32], to the T_2 mode of 2 edge-sharing $GeS_{4/2}$ tetrahedra and to the vibration of two tetrahedra connected through a bridging sulfur $S_3Ge - S - GeS_3$ [31]. The weak band near 450-500 cm^{-1} has been assigned to vibration mode of sulfur. The shoulder at around 475

#100939 - $15.00 USD Received 8 Sep 2008; revised 3 Nov 2008; accepted 7 Nov 2008; published 21 Nov 2008

cm^{-1} may be attributed to the $S_8(A_1)$ ring vibration mode of sulfur and the band at 485 cm^{-1} to the vibration of $S_n(A_1)$ chain. The bands in the range 175-225 cm^{-1} have been attributed to F_2 vibration of $GeS_{4/2}$ groups and to mixed stretching-bending vibration of Ge-S-Ge bridge bands. The structure of the as-deposited TE film is interpreted to be more connected through a larger number of $GeS_{4/2}$ units compared to the structure of the PLD film by examining the shape and intensity of the central band, most likely due to the much more energetic and rapid means by which the glass network condenses during formation. Such kinetics would freeze many more of these species present in the vapor phase, into the resulting film. Wagner *et al* showed using Laser Desorption Mass Spectroscopy that such complex entities exist in the early stages of PLD processing (in the vapor plume) and are thus likely to coalesce in the final film structure, largely unaltered [33].

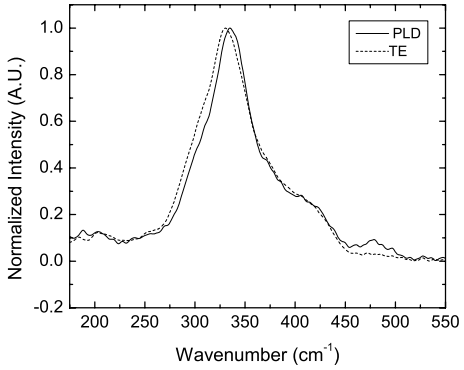

Fig. 1. Raman spectra of as-deposited films fabricated by thermal evaporation (TE) and pulsed laser deposition (PLD).

To account for the slight variation in film thickness and the expected variation in film density associated with the two deposition techniques, we can estimate the number of bonds available for interaction during exposure by comparing the differences between the two films. Here we estimate the total number of Ge-S bonds present in the laser local focal volume using the following equation:

$$\#(Ge-S) = 4 \cdot Ge_{At\%} \cdot \frac{N_A \rho}{M} \cdot V \tag{2}$$

where $Ge_{At\%}$ is the atomic fraction of Ge in the glass network (0.23), N_A is Avogadro's number, ρ is the density of the film, M the molecular weight of the glass, V the volume of the glass within focal region of the laser, and the factor of 4 results from the four-fold coordination of Ge atoms in the glass network. In this calculation, it is assumed that no homopolar Ge-Ge bonds exist in the glass matrix in accordance with the deconvolution of the Raman spectrum. The volume of glass within the focal region of the laser is calculated to be $V = \pi w_0^2 T$ to be 1.8x10^{11} and 1.3x10^{11} cm^3 for the TE and PLD films, with *T* taken to be the film thickness as 1.4±0.1 and 1.0±0.1 μm, respectively. The entire film thickness was taken to be exposure depth in the volume calculation because it was smaller than the Rayleigh length of the 0.25NA objective for these films. The densities of the films have been estimated from that of the corresponding bulk glass using the Lorentz-Lorenz equation

$$\frac{n^2-1}{n^2+2} = \frac{4\pi}{3} \cdot \frac{N_A \rho}{M} \alpha \tag{3}$$

#100939 - $15.00 USD Received 8 Sep 2008; revised 3 Nov 2008; accepted 7 Nov 2008; published 21 Nov 2008

relating the refractive index (n), density (ρ), and mean polarizability (α) [34, 35]. It is assumed that the mean polarizability of the films is equal to that of the bulk material of the same composition, though some slight density variation will be expected due to thermal history (and energy) associated with the two deposition techniques. Using a refractive index at $\lambda = 1\mu m$ of 2.14±0.02 and a measured density of 2.94±0.02 g/cm^3 for the bulk glass in Eq. (3), the mean polarizability at 1 μm has been estimated to be (3.5±0.06)x10^{-24} cm^3. Substituting the measured refractive indices at $\lambda = 1\mu m$ for the TE (2.26±0.02) and PLD (2.30±0.02) films into Eq. (3), the resulting densities of the films were determined to be 3.12±0.06 g/cm^3 and 3.17±0.06 g/cm^3, respectively. This calculation supports the expected slightly higher density of the glass deposited via a more energetic PLD process.

Inserting these density values into Eq. (2), the total number of Ge-S bonds estimated to be in the focal volume of the laser was 6.38±0.01 x10^{11} for the TE film and 4.63±0.01 x10^{11} for the PLD film. Thus, the TE film contains not only a more connected network but also a larger number of Ge-S bonds within the laser focal volume, indicating a higher susceptibility for bond modification (i.e., more bonds available to be "modified") through exposure to the femtosecond laser pulses than an identical exposure to the corresponding PLD film.

3.1 Ablation threshold of the films

The exposure values of the determined ablation thresholds for the TE and PLD films under both MHz and kHz repetition rates are shown in Table 1. When irradiated with MHz repetition rate pulses, the ablation thresholds of the TE and PLD films were measured to be 40.7±3.7 GW/cm^2 and 54.3±4.8 GW/cm^2, respectively. This indicates that the TE film is more photosensitive (undergoes changes more readily) to high repetition rate irradiation than the PLD film under comparable exposure conditions. The apparent difference in thresholds between the two types of films has been attributed primarily to increased absorption of laser light in the TE film due to a slight red shift of the band gap of the TE film compared to that of PLD film as shown in Fig. 2.

Table 1. Ablation threshold of the TE and PLD films with 1kHz and 80MHz repetition rate pulses.

Film deposition technique	198 Pulses per focal spot (1 kHz)	4x10^6 Pulses per focal spot (80 MHz)
TE	103.2 ± 0.9 TW/cm^2	40.7 ± 3.7 GW/cm^2
PLD	87.2 ± 0.9 TW/cm^2	54.3 ± 4.8 GW/cm^2

When irradiated with the kHz laser, the ablation thresholds of the TE and PLD films are about three orders of magnitude higher than with MHz exposure, increasing to 103.2±0.9 TW/cm^2 and 87.2±0.9 TW/cm^2, respectively. This observation is consistent with the expected response to energy delivered from less frequent, more largely spaced (temporally) laser pulses. Such frequency-dependent response results in higher ablation thresholds at lower repetition rates where the microsecond timescale of thermal diffusion of heat from the irradiated focal volume (as compared to the 12 ns delay between pulses with MHz exposure) results in much less cumulative heating of the glass. Thus, the reduced accumulation of thermal energy within the glass matrix results in a higher laser irradiance necessary to induce film ablation.

#100939 - $15.00 USD Received 8 Sep 2008; revised 3 Nov 2008; accepted 7 Nov 2008; published 21 Nov 2008

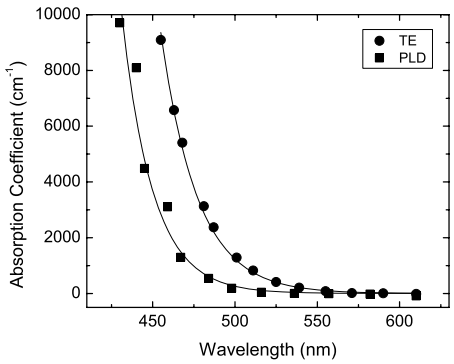

Fig. 2. Absorption spectra of the films deposited by thermal evaporation (TE) and pulsed laser deposition (PLD) techniques.

The observation that the TE film is slightly less photosensitive than the PLD in response to kHz irradiation but more photosensitive than the PLD film to MHz pulses is not fully understood, but may be related to the local matrix response to heating and interaction within the focal volume. A possible explanation for this behavior is that modification of the more highly-connected matrix of the TE film is dependent on cumulative heating by pulses with nanojoule energy at repetition rate of 80MHz and thus is not as susceptible to modification by the shot-by-shot absorption of microjoule energy pulses at a 1kHz repetition rate. While the slightly larger free volume in the TE structure may accommodate thermal-induced local distortion during higher frequency MHz shots (with limited ability to relax back when dissipating thermal energy between shots), the larger concentration of bonds means the effective absorption of heat would be larger. Additionally, the larger thickness (and thermal mass) of the TE film may result in a less efficient heat dissipation, effectively trapping the heat inside the film for a longer time and reducing the ablation threshold. Such contributions of film density (available free volume to physically distort), local thermal mass associated with focal volume bonding, all contribute to a complex interaction to the closely spaced (MHz) and more broadly spread (kHz) pulses of laser light impinging on the thin films.

3.2 Post-exposure film surface profiles – photo-expansion (ΔT)

Photo-expansion is a common result of laser irradiation in many chalcogenides. We have observed this phenomena for bulk $Ge_{23}Sb_7S_{70}$ glass [27] and for both bulk and thin film As_2S_3 glasses under NIR femtosecond laser exposure [5, 12]. Messaddeq et al have also observed an increase of the film thickness in the Ge-Ga-S and Ge-Ga-As-S glass systems with an increase of the exposure time for all powers when exposed to UV light at 351 nm [36].

In our studies, two series of photo-induced lines were written with both 1kHz and 80MHz repetition rate pulses in each type of glass film: one with varying irradiance and one with a varying number of pulses per focal spot. An examination of the surface profile using white light interferometry and AFM indicated that both exhibited localized surface photo-expansion as a result of irradiation, the magnitude of which varied as a function of both laser irradiance and number of pulses. Figures 3 and 4 illustrate the absolute magnitude (closed symbols) and normalized (open symbols) photo-expansion of the TE and PLD films as a function of the laser irradiance and the number of pulses per focal spot following kHz [Fig. 3(a) and 4(a)] and MHz exposure [Figs. 3(b) and 4(b)], respectively. As can be seen in all cases, the extent of photo-expansion increases with both an increase of laser irradiance and with the number of pulses, but the absolute magnitude as well as the expansion as a function of original thickness, is smaller in the case of kHz irradiation as compared to MHz exposed films. Additionally, PLD films show a larger extent of thickness change in the case of kHz exposure, whereas both

#100939 - $15.00 USD Received 8 Sep 2008; revised 3 Nov 2008; accepted 7 Nov 2008; published 21 Nov 2008

the TE and PLD films exhibit an almost 3% change in local thickness under MHz illumination. The photo-expansion of these samples also appears to saturate with increasing dose with MHz irradiation, as compared to the kHz irradiation, during which the photo-expansion does not saturate within the dose regime examined here. These observations can be interpreted as being related to the cumulative manner by which the local film volume is modified in the MHz exposure case and the limited volume modification that can be induced during kHz exposure case. A larger cumulative volume change observed in the case of MHz exposure suggests that local distortion of bonds and bond reconfiguration associated with laser exposure saturates after the local bonds have been fully modified. Conversely, while similar modification is thought to occur in the kHz case, the absence of heat accumulation between successive pulses limits the number of bonds modified by any given pulse. This could explain the observation that kHz irradiation results in a generally lower magnitude of photo-expansion observed by kHz irradiation that has not yet saturated within this dose regime.

3.2.1 Effect of the irradiance

Figures 3(a) and 3(b) show the evolution of the TE and PLD film surface photo-expansion as a function of the laser irradiance when irradiated with the kHz and MHz repetition rate pulses, respectively. The number of pulses per focal spot was fixed at 198 for the kHz repetition rate in Fig. 3(a) and $4x10^6$ for the MHz repetition rate in Fig. 3(b). In both figures, the magnitude of the photo-expansion increases with increasing irradiance up to the ablation threshold where higher irradiance would lead to film ablation. When exposed to kHz repetition rate pulses, the maximum photo-expansion of the TE and PLD films occurred for a laser irradiance $1.8TW/cm^2$ below the respective thresholds of each film and was measured to be 5.5 ± 0.7 nm and 10.6±0.7 nm, corresponding to a film thickness increase of 0.4±0.01% and 1.1±0.01%, respectively. The PLD film, which had a lower ablation threshold in response to kHz pulses than the TE film, had a higher photo-expansion. The photo-expansion of the two films when exposed to MHz repetition rate pulses is shown in Fig. 3(b). The magnitude of the photo-expansion is enhanced by incubation effects in the focal region of the laser, resulting in a larger photo-response that increases linearly with increasing laser irradiance until the ablation threshold. The maximum possible photo-expansion of these TE and PLD films with $4x10^6$ pulses has been estimated to be 54.4±0.7 nm and 37.8±0.7 nm, corresponding to 3.9±0.01% and 3.7±0.01%, using a linear regression in Fig. 3(b). Thus the TE film, which is more photosensitive than the PLD film when irradiated with MHz repetition rate pulses, exhibits the highest photo-expansion.

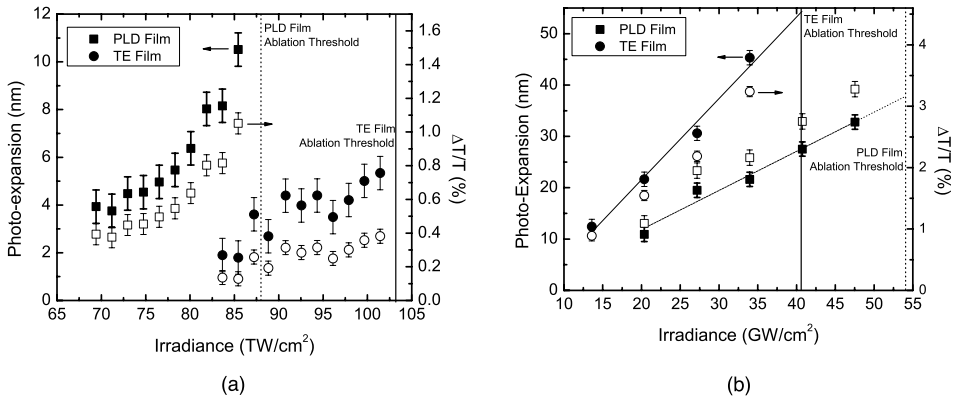

Fig. 3. Absolute (closed symbols) and relative (open symbols) photo-expansion of the investigated films when irradiated with kHz (a) and MHz (b) repetition rate pulses as a function of the irradiance. The number of pulses was fixed at 197.6 (a) and $4x10^6$ (b).

#100939 - $15.00 USD Received 8 Sep 2008; revised 3 Nov 2008; accepted 7 Nov 2008; published 21 Nov 2008

3.2.2 Effect of the number of pulses

The effect of the number of laser pulses at a fixed irradiance on the photo-expansion for both kHz and MHz pulses is shown in Figs. 4(a) and 4(b), respectively. An increase in the number of laser pulses per spot results in an increase in the height of the photo-expansion. As seen in Fig. 4(a), the PLD film exhibits a maximum photo-expansion of 9.5±0.7 nm, corresponding to a film thickness increase of 1.0±0.01% when irradiated at 85.4 TW/cm^2. In comparison, the TE film photo-expands only up to 3.7±0.7 nm corresponding to a film thickness increase of 0.3±0.01% when irradiated at a similar irradiance of 83.6 TW/cm^2. This difference in magnitude of the photo-expansion can be related to the value of the laser irradiance relative to the ablation threshold. As seen in Fig. 3, the closer the laser irradiance is to the ablation threshold, the higher the photo-expansion. Indeed, the PLD film was irradiated just below its ablation threshold, whereas the TE film was irradiated at 20 TW/cm^2 below its ablation threshold.

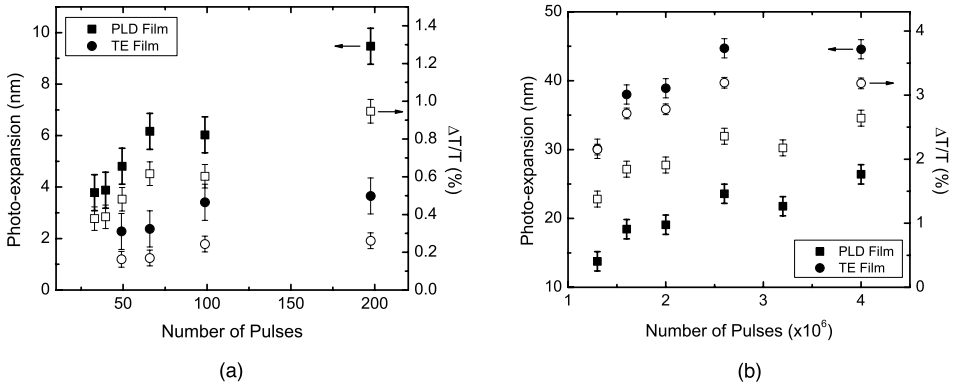

Fig. 4. Absolute (closed symbols) and relative (open symbols) photo-expansion of the investigated films when irradiated with kHz (a) MHz (b) repetition rate pulses in function of the number of pulses. The irradiance was fixed at 83.6 and 85.4 TW/cm^2 (a) and at 33.9 and 40.7 GW/cm^2 (b) for the film deposited by thermal evaporation (TE) and pulsed laser deposition (PLD), respectively.

When the repetition rate increases to 80MHz [Fig. 4(b)], the magnitude of the photo-expansion of the films increases as seen in Fig. 3. In this regime, the photo-expansion increases with increasing numbers of pulses up to about 2.6x10^6 pulses, after which the response begins to saturate. With an irradiance of 33.9 GW/cm^2 (6.8 GW/cm^2 below its ablation threshold), the TE film exhibited a maximum photo-expansion of 44.6±0.7 nm, corresponding to a film thickness increase of 2.7±0.08%. The PLD film had a smaller absolute photo-expansion, 26.4±0.7 nm, corresponding to a film thickness increase of 2.4±0.08%, when exposed with an irradiance of 40.7 GW/cm^2 (13.6 GW/cm^2 below its ablation threshold). A similar saturation effect of the surface expansion amplitude has been seen for photo-induced modifications using high repetition rate femtosecond pulses in As_2S_3 chalcogenide glasses, and may be related to a saturation of the number of free electrons available to participate in the nonlinear absorption process [5]. While the resulting laser-induced photo-expansion in these two glass systems is similar, the results shown herein show that the mechanism by which the changes occur is somewhat different (as shown in the structural changes of bond breaking/reforming in As-based glasses versus bond distortion and conformation changes in Ge-systems). It can be expected that both the electrons available to participate in the process as well as and the number/concentration of bonds available for modification will both play important roles in the resulting material modification. These results will be discussed in Section 4.

#100939 - $15.00 USD Received 8 Sep 2008; revised 3 Nov 2008; accepted 7 Nov 2008; published 21 Nov 2008

3.3 Refractive index change induced by laser irradiation – (Δn)

Understanding the femtosecond laser exposure conditions that give rise to a modification of the refractive index of a glass material is crucial to the optimization and control of the micromachining process and its use in device fabrication. The refractive index modifications to the films examined in this study have been characterized through an analysis of i) the interference fringes on the transmission spectra [29] and ii) the optical path change using a white light interferometer [5]. Both techniques yield an induced refractive index change, which includes the sign and magnitude of material changes that accompany laser exposure.

3.3.1 Transmission spectrum analysis using Swanepoel's Method

To measure the transmission spectrum of the films before and after laser irradiation, a 1.2 mm x1.2 mm square region of film was irradiated by writing parallel lines separated by 2 μm such that the dimensions of the exposed area was larger than the spectrometer beam size. It should be noted that no variation in the transmission spectrum was seen in films exposed to kHz laser irradiation with ~50 pulses per focal spot at 81.9 and 94.3 TW/cm^2, (corresponding to 5.3 and 8.9 TW/cm^2 below the ablation thresholds) for the PLD and TE films. Thus, no modification of the refractive index was seen as a result of exposure to kHz repetition rate pulses.

Figure 5(a) illustrates the transmission spectra of the TE film before and after irradiation with 34 GW/cm^2 and 1.3x10^6 pulses at 80MHz.

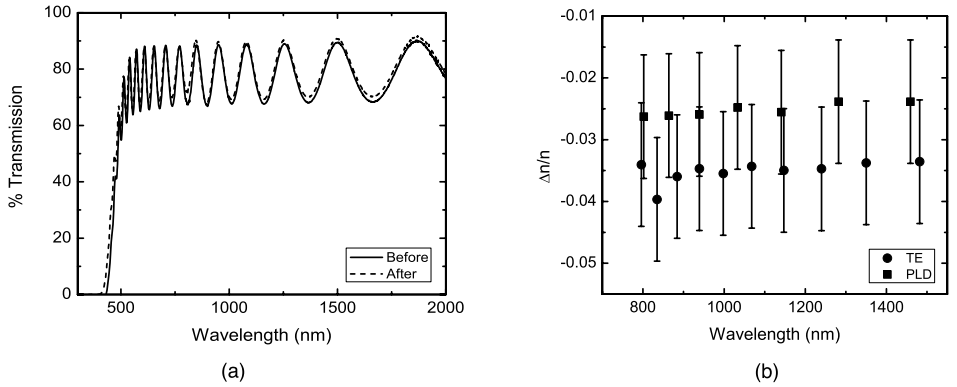

Fig. 5. (a). Transmission spectrum of the TE film before and after irradiation indicating an induced bandgap shift and a modification of the interference pattern. The laser irradiance on the sample was 34.0 GW/cm^2 (6.7 GW/cm^2 below threshold) and the number of pulses per laser spot was 1.3·10^6. (b) Δn/n of the investigated films deposited by thermal evaporation (TE) and pulsed laser deposition (PLD) as a function of wavelength.

A modification of the period of the interference fringes after irradiation is clearly visible after laser irradiation. The transmission spectra have been analyzed using the Swanepoel technique [29] and the refractive index of the film after laser irradiation was found to be lower than that of the film before irradiation, which is consistent with previous studies on laser-induced phenomena in bulk Ge-based chalcogenide glasses [37, 38]. These results are opposite in sign to index changes observed in similarly-irradiated As-based chalcogenide bulk and films. The magnitude of change of the refractive index for the TE film in this exposure regime was found to be -0.08±0.02 at 1μm as seen in Fig. 5(b). Similarly, when the PLD film was irradiated with 1.3x10^6 pulses at 40.7GW/cm^2, corresponding to exposure at a similar magnitude (13.6GW/cm^2) below its ablation threshold, the change of the refractive index was found to be -0.06±0.02 at 1μm. It is interesting to note that the normalized refractive index change Δn/n as determined by this technique in both types of film (TE and PLD), is constant

#100939 - $15.00 USD Received 8 Sep 2008; revised 3 Nov 2008; accepted 7 Nov 2008; published 21 Nov 2008

across the spectral range examined, and constant (-0.035 and -0.025) within the error of the measurement (±0.01).

3.3.2 Analysis of the optical path changes using white light interferometry

The absolute (closed symbols) and normalized (open symbols) refractive index modification of the films exposed to MHz repetition rate pulses as a function of the laser irradiance and number of pulses are shown in Figs. 6(a) and 6(b), respectively. The index change is reported at λ = 550nm as this represents the center wavelength of the white light source of the Zygo system. As shown above, the analysis shows the negative sign of the exposure-induced index change. Furthermore, the magnitude of the "decrease" in index increases with increasing irradiance and number of pulses. The maximum observed index decrease was -0.05±0.02, corresponding to a $\Delta n/n$ of 2% for both films when irradiated with $4x10^6$ pulses with an irradiance near the ablation threshold of the film. This change with dose and irradiance is consistent with changes observed for increasing irradiance and dose for film photo-expansion.

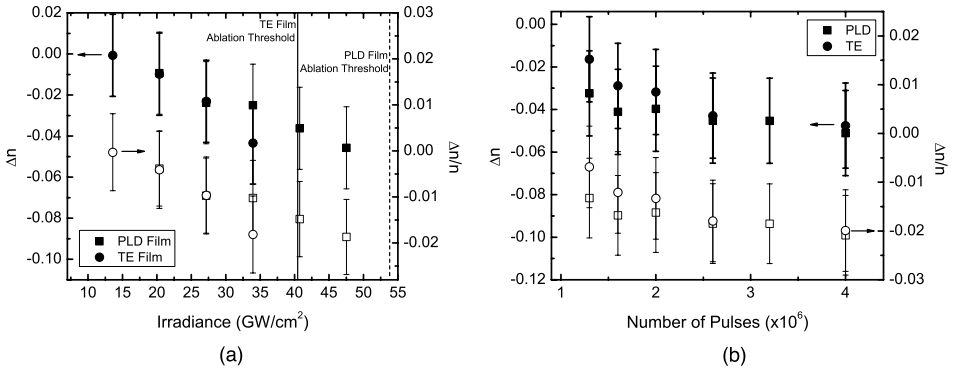

Fig. 6. Absolute (closed symbols) and relative (open symbols) refractive index modification at 550 nm of the investigated films deposited by thermal evaporation (TE) and pulsed laser deposition (PLD) techniques as a function of laser irradiance (a) and the number of pulses per focal area (b). In (a), the number of pulses per focal area was held constant at $4 \cdot 10^6$ for both films. In (b), the laser intensity was held constant at 40.7 GW/cm^2 (13.6 GW/cm^2 below threshold) for the PLD film and 34.0 GW/cm^2 (6.7 GW/cm^2 below threshold) for the TE film.

The Lorentz-Lorenz equation [Eq. (3)] indicates that the refractive index is dependent on both the density and the mean polarizability of the glass. To characterize the extent to which photo-expansion (density modification) and refractive index modification are linked, the absolute change of the refractive index, seen in the closed symbols in Fig. 6(a), was compared to the absolute photo-expansion under identical exposure conditions from the closed symbols in Fig. 3(a). These results are shown in Fig. 7 with a linear regression of the data.

#100939 - $15.00 USD Received 8 Sep 2008; revised 3 Nov 2008; accepted 7 Nov 2008; published 21 Nov 2008

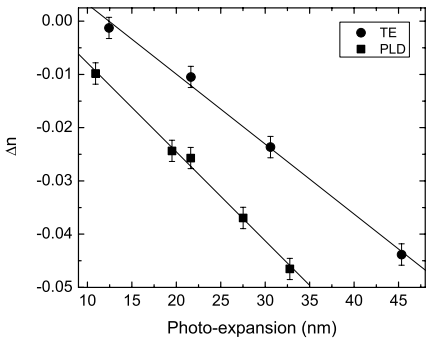

Fig. 7. Δn as a function of photo-expansion for the films deposited by thermal evaporation (TE) and pulsed laser deposition (PLD) with varying laser irradiance.

As discussed in Section 3.2, the TE and PLD film surfaces were estimated to photo-expand to a maximum of 54.4 nm and 37.8 nm respectively when exposed to $4x10^6$ pulses per focal spot with an irradiance just below their respective ablation threshold. Using the fit in Fig. 7, this corresponds to a maximum absolute change in photo-induced refractive index at 550nm for the TE of -0.066±0.02. A slightly lower Δn at 550nm of the PLD film has been determined to be -0.061 ± 0.02, which is close to that of the TE film despite the variation in deposition conditions. The linear relationship (and slopes) in Fig. 7 suggests that the induced refractive index modification is primarily due to the photo-expansion of the glass. Furthermore, the similar response for the two films suggests that the underlying mechanism responsible for the changes do not largely depend on the subtle density and bonding configuration differences associated with the film deposition techniques. This conclusion is consistent if one is to assume it is the ultimate "type" of bond and its bond strength that defines (along with secondarily the network structure) the type of photo-structural response of the glass network to laser exposure.

3.4 Proposed physical mechanism of photosensitivity

Different models of the photo-expansion effect have been proposed to explain photo-structural changes in ChG materials. Tanaka observed a volume expansion in As_2S_3 films and glasses and assumed that the volume expansion is caused by local atomic changes [39]. He also assumed that photo-induced fluidity contributes to relaxation of the local stress, giving rise to volume expansion [40]. A general mechanism for the production of photo-induced changes has been also proposed in terms of bond breaking, both intermolecular and intramolecular [41]. Following the same idea, Loeffler suggested a microscopic model in which heteropolar bonds are broken by absorption of light energy and new homopolar bonds are formed simultaneously [42]. Messaddeq *et al* correlated the volume expansion observed in Ge-Ga-S glasses to motion of chalcogen atoms into the irradiated area in particular of sulfur [36]. He also has demonstrated that the presence of oxygen is a requirement for creating a volume expansion in glasses in the system Ge-Ga-S when UV-exposed for a long period of time [43].

In the Ge-Sb-S glass system studied here, the film response to infrared (NIR) femtosecond laser light exposure produces photo-induced structural changes and property response similar to those mechanisms observed in our previous study on bulk glasses. We have shown that femtosecond laser exposure modifies the bond configuration and reorganizes the film glass' structural units by progressively decreasing the connectivity between tetrahedra units [27]. In order to understand the differences of photo-response of the TE and PLD films examined herein, micro-Raman spectroscopy has been used to characterize the photo-structural changes created by the kHz and MHz laser pulses.

#100939 - $15.00 USD Received 8 Sep 2008; revised 3 Nov 2008; accepted 7 Nov 2008; published 21 Nov 2008

3.4.1 Irradiation using the kHz laser

Figures 8(a) and 8(b) present the micro-Raman spectra of the TE and PLD film before and after laser irradiation under exposure conditions below their ablation threshold using ~200 pulses. As can be seen, no significant change in the Raman spectra of the film after irradiation exists with the exception of a slight decrease in the shoulder at 400cm^{-1} of the main band. This subtle, but repeatable change in this spectral band indicates a slight decrease in the concentration of corner sharing $GeS_{4/2}$ groups [31], presumably with a concomitant increase in edge shared species. Such a minimal conformational change in bonding within the glass network would lead to small changes in local free volume. Such a change, and the lack of significant changes of Raman spectra associated with the major backbone of the glass network, is consistent with the observation of a small (<2%) photo-expansion and no measurable refractive index modification upon kHz exposure.

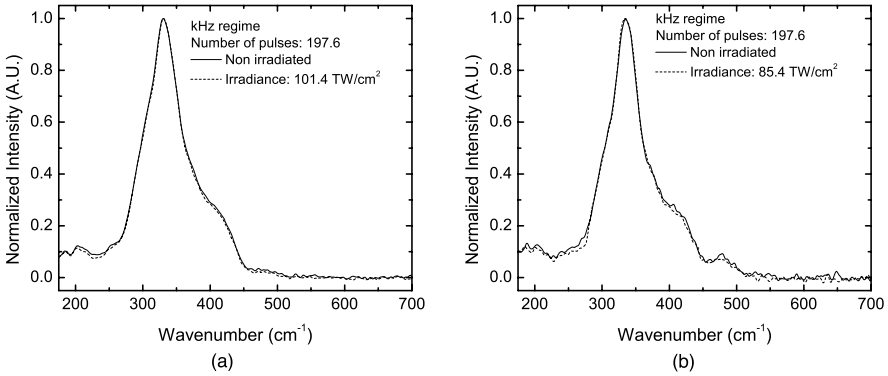

Fig. 8. Raman spectra of the films deposited by (a) thermal evaporation (TE) and (b) pulsed laser deposition (PLD) techniques before and after irradiation using kHz repetition rate pulses (λ_{exc}=785nm).

3.4.2 Irradiation using the MHz laser

Figures 9(a) and 9(b) show the micro-Raman spectra of the TE and PLD films before and after irradiation with $4x10^6$ pulses at similar exposure irradiance below their respective ablation thresholds. In order to understand the structural modification after irradiation, the main bands in the glass' spectra were deconvolved as performed in our previous study of bulk materials to resolve which bonds are being modified upon exposure [27].

#100939 - $15.00 USD Received 8 Sep 2008; revised 3 Nov 2008; accepted 7 Nov 2008; published 21 Nov 2008

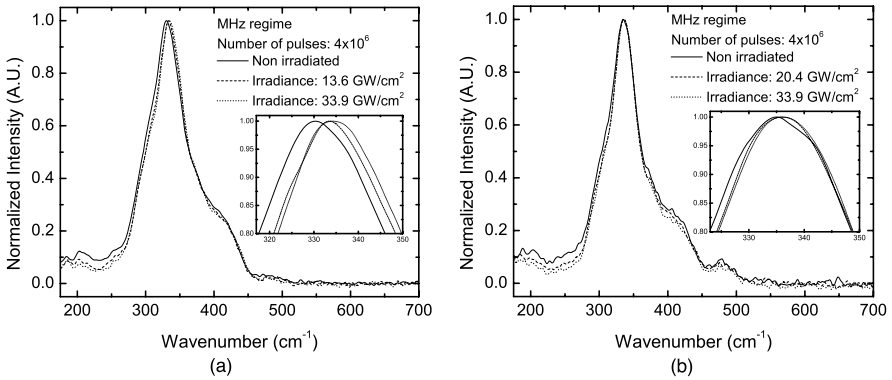

Fig. 9. Raman spectra of the film deposited by (a) thermal evaporation (TE) and (b) pulsed laser deposition (PLD) before and after irradiation using MHz repetition rate pulses with $4x10^6$ pulses incident on the sample per focal spot (λ_{exc}=785nm).

It can clearly be seen that the post-exposure Raman spectra of both the TE and PLD films exhibit similar structural modification. As the irradiance increases, the main band associated with the backbone Ge-S structural units shifts to a higher wavenumber and its bandwidth decreases slightly. The amplitude of the shoulder of the main band at ~400 cm^{-1} and of the bands at 175-225 cm^{-1} and at 450-550 cm^{-1} also decreases. The progressive shift of the main band to a higher wavenumber can be related to the progressive decrease of the shoulder at 325 cm^{-1} and the increase of the band at 338 cm^{-1}. This change indicates that the laser exposure decreases the number of the corner-sharing $GeS_{4/2}$ units and Ge-S-Ge linkages in the glass network [31], as well as contributes to a small decrease of the homopolar S-S bonds in rings and chains seen as a progressive decrease of the bands in the 450-550 cm^{-1} range. It should be noted that this modification is highly dependent on the film deposition technique as there is a much higher density of S-S linkages in the as-deposited PLD film compared to the TE film as seen by comparing the un-irradiated spectra of the two films in Figs. 9(a) and 9(b). A calculation of the integrated area of the larger S-S Raman bands in the PLD film indicates a ~26% decrease of the Raman signal upon irradiation, probably due to a decrease of S-S chains relative to rings. These structural variations suggest that the laser irradiation leads to a reduction in the connectivity of the glass network forming more isolated, less fully coordinated (each Ge would ideally have four neighbors) $GeS_{4/2}$ entities with a concomitant increase in GeS_4.

To illustrate this process, one must consider the overall network configuration. If the network of corner-connected species decreases, additional S (from S-S chains within the network) would be required to compensate charge and bonds, thus utilizing the additional S in the laser-modified network (in the creation of fully depolymerized isolated GeS_4 and partially disrupted S_3Ge-S-GeS_3 linkages which show increases in the contribution to bands at 328 cm^{-1}). Both changes are consistent with and related to the reduction in homopolar S-S units seen. It is this structural reorganization of the matrix associated with the reconfiguration the Ge-S bonds and the glass' molecular units, which can be considered responsible for the surface photo-expansion and for the decrease of the refractive index. It is also interesting to point out that as no new Raman bands appear after laser exposure, it is possible to affirm that the laser irradiation does not lead to severed bonds in the case of As-S films but rather to a modification of the bond conformation within the film network.

These qualitative changes are more fully substantiated if we quantify the photo-induced structural reorganization in the two films by estimating the number of Ge-S bonds in the various GeS_4-based units in the focal volume of the laser before and after laser irradiation. This was calculated by using the area of the deconvolved Raman bands corresponding to Ge-S

#100939 - $15.00 USD Received 8 Sep 2008; revised 3 Nov 2008; accepted 7 Nov 2008; published 21 Nov 2008

vibrational modes to calculate the relative fractions of the various types of Ge-S bonds contributing to the resulting glass structure and multiplying by the total number of Ge-S bonds within the laser focal volume calculated in Section 3. The results of these calculations associated with the Raman spectra shown in Fig. 9 with the relative fractions in brackets are summarized in Table 2.

Table 2. Total number of Ge-S bonds in different GeS_4-based structural units within the focal volume of the laser in TE and PLD films associated with Raman modifications in Fig. 9(a). The percentage of Ge-S bonds associated with the Raman bands is shown in brackets.

	TE film			PLD film		
Raman Wave-number (cm^{-1})	Unirradiated	Irradiance: 13.6GW/cm^2	Irradiance: 33.9GW/cm^2	Unirradiated	Irradiance: 20.4GW/cm^2	Irradiance: 33.9GW/cm^2
325	1.3×10^{11} [21%]	9.3×10^{10} [15%]	7.3×10^{10} [11%]	5.8×10^{10} [13%]	4.6×10^{10} [10%]	4.5×10^{10} [10%]
338	2.6×10^{11} [41%]	3.0×10^{11} [46%]	3.1×10^{11} [49%]	2.3×10^{11} [50%]	2.5×10^{11} [53%]	2.5×10^{11} [53%]
370	1.3×10^{11} [20%]	1.3×10^{11} [20%]	1.3×10^{11} [20%]	8.2×10^{10} [18%]	7.9×10^{10} [17%]	8.0×10^{10} [17%]
400	7.3×10^{10} [11%]	7.3×10^{10} [11%]	6.8×10^{10} [11%]	5.3×10^{10} [11%]	5.4×10^{10} [12%]	5.0×10^{10} [11%]
425	4.4×10^{10} [7%]	5.0×10^{10} [8%]	5.4×10^{10} [9%]	3.6×10^{9} [8%]	3.8×10^{10} [8%]	4.1×10^{10} [9%]

The decrease of the number of Ge-S bonds in $GeS_{4/2}$ units at $325cm^{-1}$ and the corresponding increase of the number of Ge-S bonds in GeS_4 at $328cm^{-1}$ [32] and S_3Ge-S-GeS_3 units at $425cm^{-1}$ [30] upon irradiation is thought to be the cause of the photo-expansion refractive index modification since both GeS_4 and S_3Ge-S-GeS_3 units are larger than $GeS_{4/2}$. Furthermore, it is clearly seen that the TE film is composed of a slightly larger number of Ge-S bonds in $GeS_{4/2}$ units, which decrease more significantly (as compared to its PLD counterpart) after laser exposure. This observation is again consistent with the observed higher photosensitivity of the TE film.

It should be noted that as observed in previously referenced studies on UV exposure of glasses in this system, no evidence of oxygen incorporation in the changes of the Raman spectra was observed after laser irradiation.

4. Conclusion

In this paper, the photo-response induced by 810nm femtosecond pulses of films with the composition $Ge_{23}Sb_7S_{70}$ deposited using both thermal evaporation and pulsed laser deposition have been studied and compared and a mechanism of bond reorganization associated with laser exposure has been proposed.

We have shown that although the films fabricated by these two techniques have the same composition, they have slightly different bond configurations and similar photo-responses, differentiated by amplitude. Due to an initially higher structural connectivity of the TE film as well as a larger number of bonds available to be modified within the focal region of the laser compared to that of the PLD film, the TE film exhibits a higher surface photo-expansion and larger induced index change, Δn, after laser exposure. It has been shown that exposure to kHz repetition rate pulses results in less than 2% surface photo-expansion with no observable index change while NIR laser exposure with the MHz laser repetition rate pulses induces surface photo-expansion up to 4% and a large (up to $\Delta n=0.10$) *decrease* in the refractive index. These physical and optical property changes have been attributed to a decrease of the glass network connectivity with the decrease of $GeS_{4/2}$ units, which occurs during light-induced conformational changes with other Ge-S units in the glass film.

#100939 - $15.00 USD Received 8 Sep 2008; revised 3 Nov 2008; accepted 7 Nov 2008; published 21 Nov 2008

The variation in magnitude of response between kHz and MHz exposure results demonstrate that the accumulation of heat associated with MHz pulses is crucial for femtosecond direct laser writing in this composition. Moreover, we have shown that the decrease of the refractive index depends on the laser irradiance and number of pulses, implying that it is possible to dynamically control the optical properties of the structures over a large range during the fabrication process. While the laser-induced refractive index change in this system is *negative* in sign and thus not suitable for waveguide writing, it is large and tailored by control of exposure repetition rate and cumulative dose. These results conclude that such engineering of glass response could be exploited to create complex, smoothly varying diffractive elements or precisely controlled features through the use of feedback.

Acknowledgment

The authors gratefully acknowledge the support of collaborators at Australian National University (B. Luther-Davies and Andre Rode) for preparing PLD films from our glasses. Funding for this work was provided by NSF (Contract # EEC-0244109), DOE (Contract # DE-FG52-06NA27502) and the State of Florida.

Disclaimer

#100939 - $15.00 USD Received 8 Sep 2008; revised 3 Nov 2008; accepted 7 Nov 2008; published 21 Nov 2008